

[©2021 IEEE](#). Personal use of this material is permitted. Permission from IEEE must be obtained for all other uses, in any current or future media, including reprinting/republishing this material for advertising or promotional purposes, creating new collective works, for resale or redistribution to servers or lists, or reuse of any copyrighted component of this work in other works.

Digital Object Identifier: [10.1109/IMFW49589.2021.9642274](#)

**2021 IEEE MTT-S International Microwave Filter Workshop (IMFW)**

### **Reconfigurable Bandpass Filter with Extracted Pole and Coupling Resonators**

Fynn Kamrath

Chad Bartlett

Patrick Boe

Daniel Miek

Michael Höft

### **Suggested Citation**

F. Kamrath, C. Bartlett, P. Boe, D. Miek and M. Höft, "Reconfigurable Bandpass Filter with Extracted Pole and Coupling Resonators," *2021 IEEE MTT-S International Microwave Filter Workshop (IMFW)*, 2021, pp. 259-261.

# Reconfigurable Bandpass Filter with Extracted Pole and Coupling Resonators

Fynn Kamrath, Chad Bartlett, Patrick Boe, Daniel Miek, Michael Höft  
 Chair of Microwave Engineering, Institute of Electrical Engineering and Information Technology,  
 Faculty of Engineering, Kiel University, Germany  
 {flk, chb, pabo, dami, mh}@tf.uni-kiel.de

**Abstract**—This paper presents a reconfigurable bandpass filter with an extracted pole section in the Ku-band. The filter’s center frequency and bandwidth can be controlled independently from each other by using additional resonators. The center frequency can be varied between 13.8 GHz and 14.8 GHz while the bandwidth can be varied between 100 MHz and 200 MHz in the given center frequency range. The extracted pole section provides a transmission zero close to the passband, which increases the selectivity and remains in place relative to the passband during all tuning states.

**Index Terms**—coupling resonators, extracted pole, reconfigurable filter, transmission zero

## I. INTRODUCTION

In recent times the frequency spectrum became a heavily contested resource and therefore efficient usage is of great importance. Furthermore, it is expected that the number of connected devices increases even further. Microwave filters are used to suppress unwanted signals, but over time, the required specification can change and therefore a variable transmission characteristic is useful. To overcome this problem, filter banks are used which consist of multiple microwave filters. These systems allow to adapt the specification to the current needs by switching to a different microwave filter. These filter banks are in general heavy and have a large footprint since they consist of multiple microwave devices. Fully reconfigurable bandpass filters are a meaningful alternative to the state-of-the-art solution since their bandwidth and center frequency can be adapted. Reconfigurable filters are able to realize different filter specifications, are more lightweight, and require a smaller footprint than filter banks. These types of filters are subject of research and have been developed in different technologies, for example, in microstrip [1], 3D printing [2], [3] and with classical milling techniques [4]. In this work, waveguide technology with the classical milling techniques are chosen since these offer a high Q-factor in the higher frequency range. The bandwidth variation is achieved through coupling resonators and a transmission zero (TZ) close to the passband is included to increase the selectivity of the filter.

This project has received funding from the European Union’s Horizon 2020 research and innovation programme under the Marie Skłodowska-Curie grant agreement 811232-H2020-MSCA-ITN-2018.

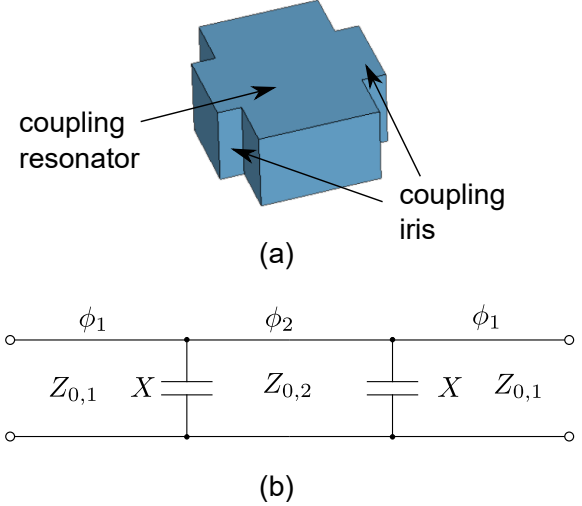


Fig. 1. Coupling resonator inverter model: (a) 3D model consisting of two identical irises and one coupling resonator and (b) equivalent circuit model

## II. COUPLING RESONATORS

This work uses so-called coupling resonators (CR) [5] to achieve full reconfigurability. The CR’s act as tunable impedance inverters and therefore allow for a change in the inverter value  $K$ . In Fig. 1, the inverter model including a coupling resonator is displayed [6]. The model consists of a non-resonating cavity, which means that the cavity is not resonating at the intended passband, between two identical irises. The characteristic impedance is represented by  $Z_0$  while  $\phi_1$  represents the loading effects on the adjacent resonators. These influence their resonance frequency by shortening their electrical length. The electrical length of the coupling resonator is represented by  $\phi_2$  and varies depending on its resonance frequency. By adjusting the coupling resonator’s resonance frequency the inverter value  $K$  changes and the coupling strength can be adapted to a different value. In this work tuning screws are used to allow for a continuous reduction of the resonance frequency by inserting the screw deeper inside the cavity. This can be used to change the inverter value  $K$  and therefore the inter-resonator coupling continuously.

For the design, the external quality factor  $Q_e$  can be

calculated by:

$$Q_e = \frac{\omega_0}{\Delta\omega_{3dB}}, \quad (1)$$

where  $\Delta\omega_{3dB}$  is the 3 dB bandwidth. To calculate  $Q_e$  the first main resonator and both adjacent coupling resonators have to be simulated, while having a weak coupling at the load port [7]. The influence of coupling resonators on the bandwidth can be explained using (2), which can be applied for inter-resonator coupling with in-line topologies:

$$\frac{K_{i,i+1}}{Z_0} = \frac{\pi\Delta}{2\sqrt{g_i g_{i+1}}} \quad \text{for } i = 1, \dots, n-1, \quad (2)$$

where  $\Delta = \frac{\lambda_{g1} - \lambda_{g2}}{\lambda_{g0}}$ . In (2), the connection between the inverter value  $K$ , the  $g$ -values, and the guide wavelengths is displayed [8]. The bandwidth of the filter is related to  $\Delta$ , since the guide wavelengths  $\lambda_{g1}, \lambda_{g2}$  are calculated at the lower and upper band-edges of the passband. The  $g$ -values are dependent on the chosen topology and return loss level of the filter and remain static. Therefore, a change in the inverter value  $K$  causes a shift of the passband edges. Furthermore, by using coupling matrix extraction, the coupling values can be calculated as well. For a fully reconfigurable filter, CR's have to be placed adjacent to each main resonator to be able to adapt each coupling individually.

### III. FILTER DESIGN

The filter is designed to be tunable between 13.9 GHz to 14.9 GHz and bandwidth tunable between 100 MHz to 200 MHz. A third order filter is chosen as a trade off between complexity and increased selectivity. Therefore, the filter consists of three main resonators, which form the passband, four coupling resonators, which control the external/inter-resonator coupling and one non-resonating node (NRN) to couple the the center resonator in an extracted-pole topology for the generation of a TZ. The NRN is positioned in the center of the filter which allows for a symmetrical structure. The irises adjacent to each coupling resonator are symmetrical, which further reduces the design complexity. Tuning screws are used in the center of each resonator to influence its resonance frequency, with exception of the NRN. For the same center frequency, the transmission zero only moves  $\approx 10$  MHz relative to the passband edge depending on the bandwidth.

The coupling resonators can be dimensioned to resonate either below or above the passband [5], [9]. In the presented structure, the coupling resonators as well as the NRN operate below 13 GHz to not disturb the passband. The closer the coupling resonator's resonance frequency is to the passband, the stronger the inter-resonator coupling. For low bandwidth configurations, the resonance frequencies of the coupling resonators are pushed below 12.25 GHz since a weak coupling is needed. The first higher order mode of the NRN and the CRs is occurring above 17 GHz and 18 GHz, respectively, which leaves the range from 13 GHz to 17 GHz without spurious resonances. The higher order mode of the NRN is not influenced by any tuning screws which causes the resonance to remain in place during all tuning states.

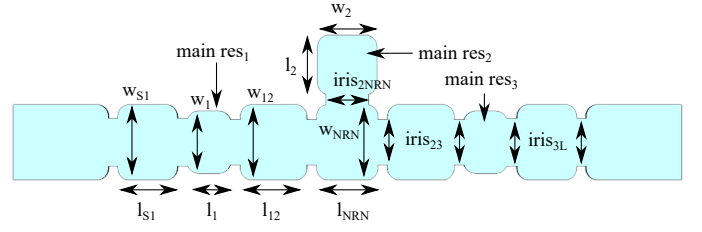


Fig. 2. Top down view of the filter structure. Dimensions in mm:  $l_{S1} = 12.5$ ,  $l_1 = 9.25$ ,  $l_{12} = 14$ ,  $l_{NRN} = 12.9$ ,  $l_2 = 12.5$ ,  $w_{S1} = 15.79$ ,  $w_1 = 13$ ,  $w_{12} = 15.79$ ,  $w_{NRN} = 15.79$ ,  $w_2 = 12.5$ ,  $iris_{2NRN} = 9$ ,  $iris_{23} = 9.5$ ,  $iris_{3L} = 10$ . The filter is symmetrical in relation to the NRN. The blend radii are 2 mm.

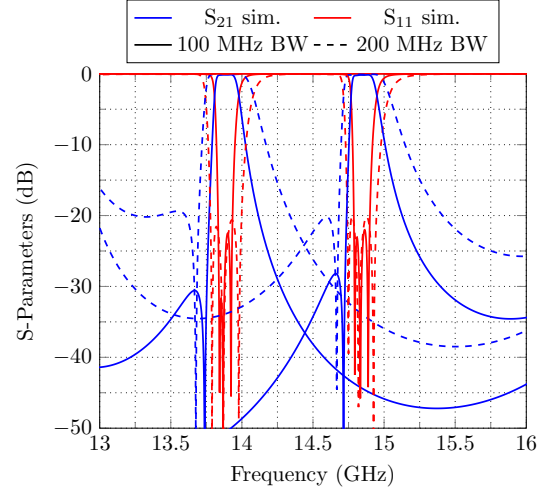


Fig. 3. Simulation results of different tuning states.

The main resonators are dimensioned in order to resonate slightly above the highest desired passband frequency. This is used as a safety margin since the coupling resonators have a small influence on the main resonator's resonance frequency. In this manner, different tuning states have slightly different effects on the main resonators. The widths and lengths of the main resonators are modified to approach a square footprint which results in a higher Q-factor. In the case of main resonator 1 and 3, their widths are reduced to approach these optimal dimensions while resonator 2 is completely square.

After each resonator is dimensioned properly, the iris widths have to be adapted so that the desired coupling strength for a tuning state is achieved. The complete filter structure and the final dimensions can be seen in Fig. 2. The main resonators, which form the passband, are marked separately, while the larger cavities are the coupling resonators. In Fig. 3 the simulation results for different center frequency and bandwidth configurations are displayed.

### IV. MEASUREMENT RESULTS

The filter is manufactured out of aluminum without silver plating and is shown in Fig. 6. Recesses are foreseen to increase the pressure on the cavity edges to improve the electrical connection. In Fig. 4, the measured response for a upper

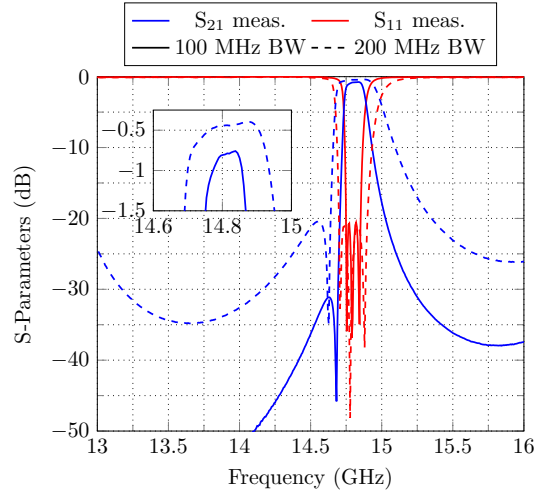


Fig. 4. Measured filter response for a center frequency of 14.8 GHz.

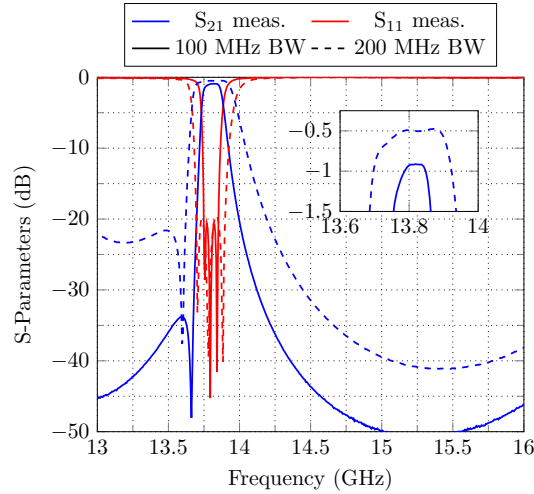


Fig. 5. Measured filter response for a center frequency of 13.8 GHz.

Ku-band center frequency is displayed. The filter was designed to achieve a maximum center frequency of 14.9 GHz while the measurements reveal a small reduction to 14.8 GHz, which might be related to manufacturing inaccuracies. The insertion losses (IL) for each of the tuning states are  $IL \geq 0.4$  dB and  $IL \geq 0.75$  dB, respectively. This results in a Q-factor of  $Q_u \approx 2000$ . The tuning states at a lower center frequency suffer from slightly higher insertion losses with  $IL \geq 0.5$  dB and  $IL \geq 0.91$  dB since the tuning screws have to be inserted deeper into the cavities. At all tuning states, a return loss above 20 dB can be achieved. In Fig. 4 and Fig. 5, only the edge cases are shown, as the coupling strength can be varied continuously. In the range from 13.8 GHz to 14.8 GHz, any bandwidth between 100 MHz and 200 MHz can be realised with a return loss of at least 20 dB.

## V. CONCLUSION

In this paper, a reconfigurable bandpass filter with an extracted-pole section is presented. The filter structure utilizes

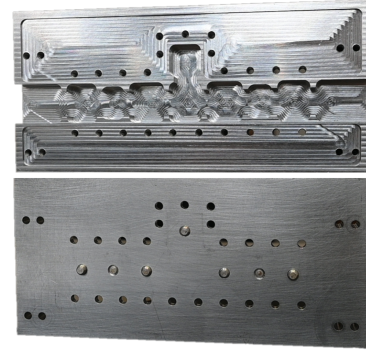


Fig. 6. Photo of the manufactured reconfigurable filter with extracted pole. Top: filter with cavities Bottom: top cover

coupling resonators to realize different bandwidths. The extracted pole provides a transmission zero close to the passband to offset the influence of the coupling resonators operating below its center frequency and to increase the selectivity. The filter is manufactured out of aluminum and the simulation results are verified. A good agreement between simulation and measurements can be seen although a frequency shift is noticeable, which can be attributed to small manufacturing inaccuracies. The presented filter achieves a Q-factor of  $Q_u \approx 2000$ , which is slightly lower during tuning states with a lower center frequency.

## REFERENCES

- [1] C. Schuster, F. Kamrath, D. Miek, E. Polat, P. Boe, L. P. P. Frank, D. Kienemund, R. Jakoby, H. Maune, and M. Höft, "Fully reconfigurable bandpass with continuously tunable center frequency and bandwidth featuring a constant filter characteristic," in *2020 German Microwave Conference (GeMiC)*, 2020, pp. 236–239.
- [2] N. Jolly, O. Tantot, N. Delhote, S. Verdeyme, L. Estagerie, L. Carpentier, and D. Pacaud, "Wide range continuously high electrical performance tunable e-plane filter by mechanical translation," in *2014 44th European Microwave Conference*. IEEE, Oct 2014.
- [3] A. Perigaud, O. Tantot, N. Delhote, S. Bila, S. Verdeyme, and D. Bailargeat, "Continuously tunable filter made by additive manufacturing using a 3d spiral ribbon," in *2017 IEEE MTT-S International Microwave Workshop Series on Advanced Materials and Processes for RF and THz Applications (IMWS-AMP)*. IEEE, Sep 2017.
- [4] U. Rosenberg, R. Beyer, P. Kraus, T. Sieverding, A. Papanastasiou, M. Pueyo-Tolosa, P. M. Iglesias, and C. Ernst, "Reconfigurable doublet dual-mode cavity filter designs providing remote controlled center frequency and bandwidth re-allocation," in *2016 46th European Microwave Conference (EuMC)*. IEEE, Oct 2016.
- [5] C. Arnod, J. Parlebas, and T. Zwick, "Center frequency and bandwidth tunable waveguide bandpass filter with transmission zeros," in *2015 European Microwave Conference (EuMC)*. IEEE, Sep 2015.
- [6] C. Arnold, J. Parlebas, and T. Zwick, "Reconfigurable waveguide filter with variable bandwidth and center frequency," *IEEE Transactions on Microwave Theory and Techniques*, vol. 62, no. 8, pp. 1663–1670, 2014.
- [7] J.-S. Hong and M. J. Lancaster, *Microstrip filters for RF/microwave applications*. John Wiley & Sons, Inc., Jun 2001.
- [8] R. J. Cameron, C. M. Kudsia, and R. R. Mansour, *Microwave filters for communication systems*. John Wiley & Sons, Inc., 2018.
- [9] F. Kamrath, D. Miek, P. Boe, and M. Höft, "Fully reconfigurable bandpass filter with coupling resonators and arbitrary transmission zero position," in *2020 IEEE Asia-Pacific Microwave Conference (APMC)*. IEEE, Dec 2020.